Towards Universal Haptic Library: Library-Based Haptic Texture Assignment Using Image Texture and Perceptual Space

Waseem Hassan ^{ID}, Arsen Abdulali ^{ID}, Muhammad Abdullah,
Sang Chul Ahn ^{ID}, *Member, IEEE*, and Seokhee Jeon, *Member, IEEE*

Abstract—In this paper, we focused on building a universal haptic texture models library and automatic assignment of haptic texture models to any given surface from the library based on image features. It is shown that a relationship exists between perceived haptic texture and its image features, and this relationship is effectively used for automatic haptic texture model assignment. An image feature space and a perceptual haptic texture space are defined, and the correlation between the two spaces is found. A haptic texture library was built, using 84 real life textured surfaces, by training a multi-class support vector machine with radial basis function kernel. The perceptual space was classified into perceptually similar clusters using K-means. Haptic texture models were assigned to new surfaces in a two step process; classification into a perceptually similar group using the trained multi-class support vector machine, and finding a unique match from within the group using binarized statistical image features. The system was evaluated using 21 new real life texture surfaces and an accuracy of 71.4 percent was achieved in assigning haptic models to these surfaces.

Index Terms—Perceptual space, multi-dimensional scaling, image features, psycho-physics

---

1 INTRODUCTION

ONE of the imminent bottlenecks in current haptics technology for virtual reality (VR) is the difficulty of haptic modeling. Haptic feedback in a virtual environment usually requires a geometric model of the environment as well as haptic property models associated with the geometry [1]. For geometry modeling, many available tools, resources, and algorithms for computer graphics can be utilized for haptic modeling since a single geometric model is usually shared. However, models for haptic properties, e.g., stiffness, friction, surface texture, are much harder to obtain. Modeling usually involves manual tuning of parametric models, e.g., [2], [3], [4] or training of non-parametric interpolation models, e.g., [5], [6], [7].

One of the emerging techniques for haptic modeling is the data-driven haptic modeling [8], [9], [10], [11]. In this technique, the signals originating from tool-surface interaction are recorded, e.g., high frequency vibrations generated by stroking a surface. These signals are subsequently used in rendering for approximation of the given surface. Based on data-driven modeling, the authors in [9] recorded the normal force and scanning velocity during interaction and rendered realistic isotropic haptic textures using that information. Similarly, more complex anisotropic textures were modeled and rendered in [12], [13] by including the direction of scan velocity along with normal force in the input data. One of the reasons for the huge popularity of data-driven modeling is that the model is created directly from interaction data regardless of the object properties or micro geometry of the surface. In case of manual tuning, these factors significantly influence the modeling and thus make it a cumbersome task.

Another positive aspect of data-driven modeling is the ease in generation of data. The model is captured by stroking a given surface and quality of the model is determined by comparing the error between the rendered and actual signal. On the other hand, the services of an expert are always required in manual tuning. All the parameters of the model have to be manually examined or felt by an expert or a designer and tuned according to the given surface.

With the introduction of data-driven technique, haptic modeling has become significantly robust but there still remain some underlying problems that render model making a difficult task. First, every object has to be somehow probed by a sophisticated sensing hardware to get data for modeling. Data-driven modeling is efficient in comparison with manual tuning, but it can still take a lot of time and effort to model a significantly large number of surfaces. For example, modeling all the surfaces in a complex virtual reality environment (e.g., 3D gaming environment) can prove to be a difficult task using data-driven modeling. Second, as it is evident that an object needs to be physically present in order to be modeled. Certain scenarios can arise where

---

- W. Hassan, A. Abdulali, M. Abdullah, and S. Jeon are with the Department of Computer Science and Engineering, Kyung Hee University, Seoul 130-701, Republic of Korea. E-mail: {waseem.h, abdulali, abdullah, jeon}@khu.ac.kr.
- S. C. Ahn is with the Imaging Media Research Center, Korea Institute of Science and Technology, Seoul 02792, Republic of Korea. E-mail: asc@imrc.kist.re.kr.
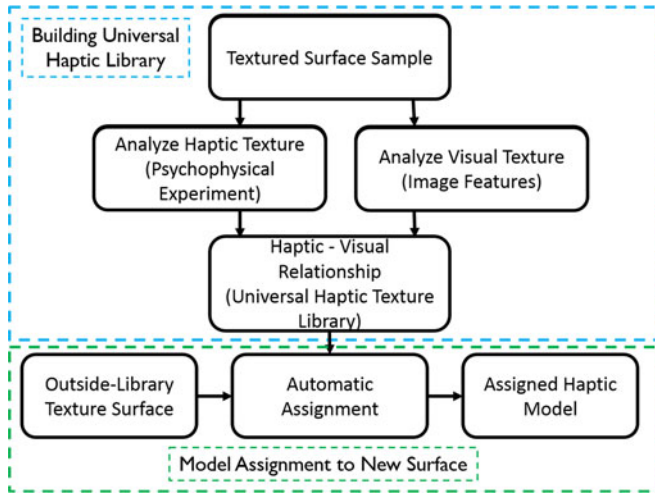
Fig. 1. Overall framework of haptic library and automatic assignment.

modeling an object without physical presence may be required. One such instance can be modeling all the fabrics in an online shopping outlet. Keeping these shortcomings in mind, we need to develop a method where haptic modeling is more robust, easy to adapt to new surfaces, and detached from dependence on physical presence of the objects.

Another difficulty in haptic modeling is the association of haptic property models with the geometry. Currently, such property authoring is usually done manually by a haptic programmer directly in a rendering program code, e.g., openHaptics and CHAI3D. Some efforts exist for providing an intuitive tool for haptic authoring, e.g., [14], [15], but manual assignment and tuning still takes some efforts.

Our research thrust is originated from the need of efficient haptic modeling. The broad goal of the current research is to build a "Haptic texture library" – a collection of a large number of haptic models that describe a wide range of haptic surfaces - and to develop a method that automatically authors the haptic property of the environment with minimal effort using the library. We hope that with this tool, application-ready and haptic-enabled environment models can be easily generated without extensive modeling.

As one of the attempts towards this goal, this paper proves the concept of image texture-based automatic assignment with focus on haptic texture. It is reported that haptic texture has, up to some extent, correlation with image texture [16], [17], [18]. However, it is also well known that two similar looking surfaces can have totally different haptic perceptions. This indicates that pure image-based texture classification techniques may fail to distinguish surfaces with different haptic feelings. Although images can be misleading at times, but there definitely exists an overlap in the information conveyed through visual and haptic cues, as mentioned earlier. This paper uses that information to cater for the perception aspects of every image and use it in automatic assignment of haptic texture models. The main purpose of adapting this image based approach is to make the process of haptic modeling more robust, intuitive, and easy to implement and generalize.

The overall framework required to accomplish this task can be tabulated as follows:

1 -   One time data driven modeling of texture surfaces to form a library. The range of surfaces should cover most of the daily life haptic interactions.

2 -   A user study to establish a perceptual space where all the surfaces from the library are represented based on their perceptual characteristics of haptic texture.

3 -   Extract image features of all the texture surfaces.

4 -   Establish a relationship between haptic perception (step 2) and image features (step 3). Haptic texture models and image features are stored together.

5 -   Based on the relationship established in step 4, carry out automatic haptic texture model assignment to newly encountered - outside library - texture surfaces, using the library.

6 -   Render the assigned model from library as a haptic model for the newly encountered texture surface.

Data driven modeling and rendering are not addressed here due to scope of the article. However, the details of the modeling and rendering techniques used in the current study can be found in [12] and [13], respectively. The three dimensional input space (2-d velocity and 1-d force) in [12] and [13] has been reduced to a two dimensional one (1-d velocity and 1-d force) for handling the isotropic surfaces used in this study. Focus of the present paper lies in the process of automatic assignment, i.e., steps 2 - 5. The overall framework for automatic assignment is provided in Fig. 1.

The steps associated with automatic assignment are addressed in the following sections. Perceptual space is established in Section 3. Section 4 is dedicated to extraction of image features and selection of the image features which best describe the perceptual space. The Relationship between image feature space and perceptual space is discussed in Section 6. Furthermore, the evaluation of the proposed system is carried out in Section 7. The discussion, based on the results, is given in Section 8. The paper is concluded in Section 9.

1.1   Contributions

The major contributions of this study are listed below:

○   Establishing a perceptual space by conducting a psychophysical experiment with 84 real life textured surfaces.

○   Establishing a universal haptic texture library where the 84 surfaces are stored along with their associated image features.

○   Proposing an automatic assignment algorithm for haptic texture model assignment, which can be readily used to assign data-driven haptic models to textured surfaces based on their images only.

1.1.1   Expected Outcomes

The shortcomings in data-driven modeling mentioned in the above section can be overcome by adapting automatic assignment algorithm. First, since the assignment calculates image features from the new surface and then selects an appropriate model based on those image features, haptic models can be assigned to a large number of new surfaces in a very short time (within seconds) using the automatic assignment algorithm. This process takes far less time as

compared to physically interacting with a large number of surfaces and modeling them.

Second, haptic models are assigned using only images of the new surfaces. This eliminates the need for physical presence of the target object or surface. The significance of this technique is that we can render surfaces which are not physically available, such as the online shopping example discussed earlier or a 3D gaming environment.

Association of haptic property models with geometry can also be achieved using the proposed algorithm. Although it is not addressed in the manuscript, the concept is quite straightforward to apply. Assume a mesh model with surface texture. A haptic model can be assigned to each vertex (or group of vertices) based on the surrounding texture. Such an approach can alleviate the need for manual assignment or tuning. Furthermore, a variety of 3D mesh models along with textures are available. These can easily be assigned haptic models based on the proposed algorithm.

1.2 Limitations

The proposed algorithm has been developed by applying certain assumptions and restrictions which must be kept in mind to achieve correct classification results. These assumptions and restrictions are detailed below.

- ○ The resolution of the image used for classification must be high enough to reveal surface topography.
- ○ Only natural textures should be used as synthetic textures can provide misleading image features.
- ○ The proposed algorithm does not consider stiffness of the surfaces for classification purposes.

2 BACKGROUND

This section covers three different aspects of literature. The first part deals with the perceptual dimensions of haptic texture, the second part briefly elaborates the relationship between visual and haptic texture, while the third part details the previous techniques used for texture classification.

2.1 Perception of Tactile Textures

Interaction with textured surfaces can occur in two ways: tool-based or bare-handed. Both these types of interactions have received a lot of attention from the research community. In case of bare-handed interaction, the researchers have focused on finding the underlying factors or perceptual dimensions that contribute towards the haptic texture perception. Yoshida et al. [19] were among the first in finding the perceptual dimensions for bare-handed interaction. They reported four main dimensions for haptic texture, i.e., hard-soft, heavy-light, cold-warm, and rough-smooth. Hollins et al. used bipolar adjective scales to define the basic dimensions in [20]. They identified smooth-rough and soft-hard as the two main dimensions in haptic texture perception. In summary, as corroborated by [21], haptic texture perception mainly consists of three basic dimensions, i.e., rough-smooth, hard-soft, and cold-warm (e.g., [22], [23]). However, authors in [21] provide reasonable grounds to include friction as another dimension to cater for the stickiness-slipperiness of surfaces and that roughness dimension can be divided into macro and micro roughness. On the other hand, for tool-based interaction, Lamotte, in [24], showed that texture perception varies along the hard-soft dimension. It was concluded that participants were better at discriminating the differences in softness when they used active tapping. Other studies such as [25], [26] found that textural perception varies along the rough-smooth dimension.

2.2 Visual and Haptic Texture

When a person looks at an object while investigating it with hands, vision and haptics provide information about the characteristics of that object. Vision mostly dominates the information about shape, color, position, etc., while haptics provide richer information regarding texture [17], [27]. Contrary to popular belief, S.J. Lederman et al. and M.A. Heller showed, in separate studies, that vision and haptics perform equally well in texture perception tasks [16], [27]. In fact, it was argued that texture perception is intrinsically a bimodal (visual and haptic) phenomenon and perception degrades if observed through either of the individual modalities. Furthermore, functional Magnetic Resonance Imaging (fMRI) based studies showed that the two modalities are not independent and provided evidence of a crossmodal interaction in the visual and somatosensory cortices when texture information is processed [17]. Dominance of a particular modality in a texture perception task is governed by the amount of variance in the information available to that modality. To this end, Ernst et al. modeled the human nervous system responses using a maximum-likelihood integrator which accepted visual and haptic cues as inputs and estimated the role of each modality in perception [18]. All the above studies and numerous others suggest that visual and haptic texture perception operate in a flexible cooperation and that there exists a common ground between them. In this study we exploit this common ground to associate visual information from images with haptic information in the form of haptic texture models.

2.3 Haptic Texture Classification

A variety of studies have focused on images of materials for surface texture classification. These studies differ mainly in the kind of image features used for classification. One of the earliest efforts in this area was provided by Haralick et al. [28]. They used various features extracted from Grey Level Co-occurrence Matrix (GLCM) for surface classification. Others followed suit and calculated different features from the image intensity values. In [29], the authors used the GLCM features for color texture classification. Various other studies used local binary pattern features [30], filter bank features [31], binarized statistical image features [32] etc, for texture classification. One of the major hindrances in using these techniques for haptic texture classification is that the classification is purely image based and as such cannot be directly applied to haptic texture classification.

One of the emerging methods for texture classification in the field of haptics is classification based on the vibration signals originating from tool-surface interaction. The tool is loaded with various sensors to record different aspects of the interaction, i.e., scanning velocity, normal force, friction etc. Stresse et al. [33] recorded acceleration signals originated during free-hand exploration of texture surfaces. Afterwards, well-known audio features were extracted from the
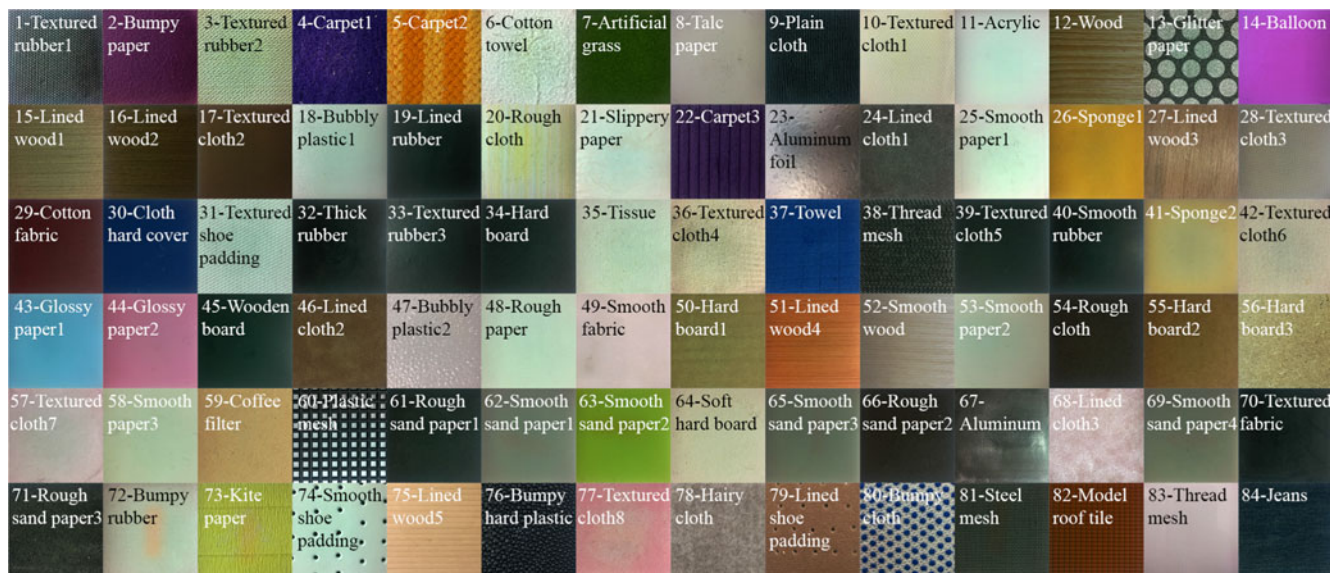
Fig. 2. Eighty-four real-life texture samples used in this study.

signals and used for classification and recognition of texture surfaces. In addition to accelearation, Romano et al. [34] also used the normal force, scanning velocity, and frictional force experienced during the interaction. They modified the vibration according to the human perception by binning the frequency domain on a non-linear scale. They achieved high texture recognition rates despite varying physical contact conditions by using a multi-class support vector machine (MC-SVM). In [35], the authors used a custom built pen to captured the acceleration, sound, frictional force, and images of the surface during interaction. These data were used to record six features for surface classification.

The common denominator among the above mentioned studies is the physical acceleration signals and other mechanical properties captured during tool-surface interaction. It can be argued that features based on the mechanical properties produce haptically better classification results. However, generalizing this method to modeling outside-library texture surfaces still remains a problem as it requires interaction with the physical surface. Using the proposed method, haptic model to an outside-library texture surface can be assigned based only on the image of that particular surface. Thus the current study enhances the robustness and usability of the haptic modeling process.

3 PERCEPTUAL HAPTIC TEXTURE SPACE

In the perceptual haptic texture space, real life textured surfaces are represented as points in an n-dimensional perceptual space. We use Multidimensional Scaling (MDS) analysis to represent the perceived texture of a textured surface. Each surface is represented as a point in the perceptual space. The distances among the textured surface locations are chosen such that they represent the perceived dissimilarity between them. A psychophysical experiment was conducted to find the dissimilarities between various real life textured surfaces.

3.1 Establishing Perceptual Space

A cluster sorting experiment was carried out to find the dissimilarities between the real life textured surfaces. The

authors in [36] show that cluster sorting can accurately capture the dissimilarity data. This dissimilarity data was used to establish the haptic perceptual space.

3.1.1 Participants

A total of ten participants took part in the experiment. They were paid for their participation. Their ages ranged from 22 to 31 years. The participants reported no disabilities and had little or no expertise regarding the experiment.

3.1.2 Stimuli

The experiment consisted of 84 different real life textured surfaces. These 84 textured surfaces were subjectively selected in such a way that they captured the whole range of daily life haptic interactions that happen in a common office. The textured surfaces were glued to rigid acrylic plates of size $100 \times 100 \times 5$ mm. The real life textured surfaces will be referred to as 'samples' from here on for convenience. The details of all the textured surfaces can be found in Fig. 2.

It should be noted that the participants were asked not to judge the surfaces based on differences in stiffness, because, all the surfaces were mounted on hard acryl plates which augmented the actual stiffness of all the surfaces. Excluding stiffness, all the other haptic properties were considered for clustering the given surfaces.

3.1.3 Procedure

A table was placed in front of the participants. Instructions to the participants were provided on a printed piece of paper. After reading the instructions, the participants were encouraged to ask questions regarding the experiment. The participants wore a blindfold to restrict visual cues during the experiment. The participants also wore headphones playing pink noise. The volume of the pink noise was controlled such that it masked the sound of interaction of hand with the sample, while not obstructing normal conversation. The experimental setup is shown in Fig. 3.

The experiment was a cluster sorting task similar to the one carried out in [36], [37]. Participants were asked to

Fig. 3. Experimental setup for the cluster sorting task.

Fig. 5. Kruskal stress values for the first ten dimensions of the 84-surface and 105-surface perceptual spaces.

sort the 84 samples into predefined number of groups. They were asked to assign a given sample to a group based on the similarities with other samples in that particular group. A total of five trials were conducted per participant. The total number of groups in the five trials were 3, 6, 9, 12, and 15, respectively. The order of trials was changed across participants to remove ordering bias. The total number of groups across trials were varied because, on one hand, a lower number of groups per trial ensured a broader classification of the samples, while, on the other hand, a higher number of groups ensured that the samples were classified more precisely. This ensured that the trials with lower number of total groups helped in forming major groups in the sample set. The samples having a vague perceptual resemblance were grouped together. While, the trials with higher number of total groups helped in gathering very similar samples into the same groups, thus, providing groups with perceptually very similar samples. The participants were free to use any exploring strategy while interacting with the samples with their bare-hands. Once all the samples were classified, the participants were given a second chance to check all the groups for any errors in classification. In case of an error, they were allowed to assign it to a new group. The participants were allowed to take short breaks of five to ten minutes between trials. On average the experiment took 150 minutes per participant excluding the break times.
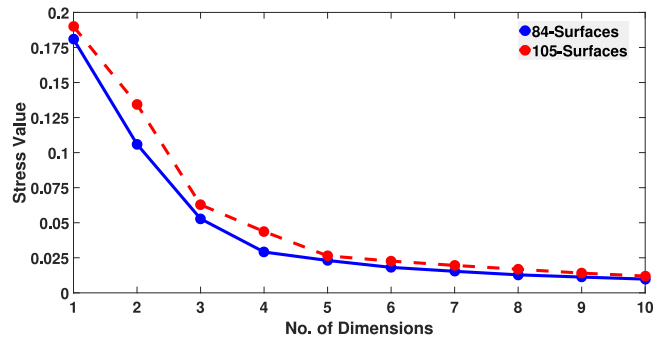
3.1.4 Data Analysis

To convert the data into meaningful information, a similarity matrix was formed from the similarity scores of all the individual samples. Score to a pair of samples was assigned based on the total number of groups present in that particular trial, and subsequently, the scores across all the trials were added. For example, if a pair of samples was grouped together in the trials with total number of groups at 3, 6, and 9, then the total score for that pair would be 3 + 6 + 9 = 18. The sample pairs which were perceptually very similar would be grouped across most of the trials and thus obtaining a higher similarity score. This data was used to form a similarity matrix for all the participants. Afterwards, the similarity matrix was converted to a dissimilarity matrix , scaled from 0 to 1000, and averaged across all participants.

3.1.5 Results

Using the average dissimilarity matrix, non-metric MDS analysis was performed. Based on the Kruskal stress [38], a three dimensional representation was selected for the perceptual space. The stress value at dimension three is 0.05, which is considered as fair according to [39]. Furthermore, the decrease in stress values after dimension three is relatively small. The three dimensional MDS scatter graph of the perceptual space and the Kruskal stress for the first ten dimensions are shown in Fig. 4, and 5, respectively.
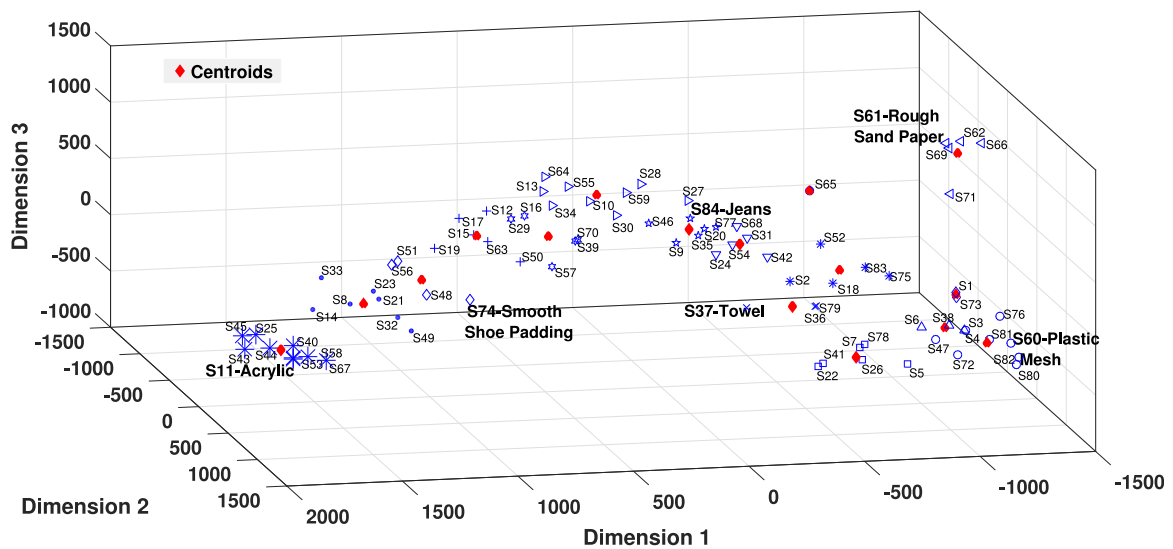

Fig. 4. Three dimensional MDS of perceptual space. The different shapes represent the different groups as a result of K-means clustering. The filled red diamonds show the centroids of the groups.

TABLE 1
List of All the Image Features Used to Establish the Image Feature Space

GLRLM Features [40], [41], [42], [43]	GLCM Features at d = 1,2,4 [28], [44]	
Short Run Emphasis	Sum of Squares	Energy
Long Run Emphasis	Sum Average	Entropy
Gray-Level Nonuniformity	Sum Variance	Dissimilarity
Run-Length Nonuniformity	Sum Entropy	Contrast
Run Percentage	Difference variance	Cluster Prominence
Low Gray-Level Run Emphasis	Difference entropy	**Correlation**
High Gray-Level Run Emphasis	Maximum probability	**Homogeneity***[*]
Short Run Low Gray-Level Emphasis	**Information measures of correlation (1)**	Autocorrelation
Short Run High Gray-Level Emphasis	**Information measures of correlation (2)**	Cluster Shade
Long Run Low Gray-Level Emphasis	**Inverse difference moment normalized**	
Long Run High Gray-Level Emphasis		
Gray-Level Variance		
Run-Length Variance		
GLSZM Features [40], [41], [42], [43]	**NGTDM Features** [45]	**Gradient Features**
Small Zone Emphasis	Coarseness	Non-Zero
Large Zone Emphasis	Contrast	Kurtosis
Gray-Level Nonuniformity	Busyness	Skew
Zone-Size Nonuniformity	Complexity	Percent 1
Zone Percentage	Strength	**Percent 25**
Low Gray-Level Zone Emphasis		Percent 50
High Gray-Level Zone Emphasis		Percent 75
Small Zone Low Gray-Level Emphasis		Percent 90
Small Zone High Gray-Level Emphasis		Percent 99
Large Zone Low Gray-Level Emphasis		
Large Zone High Gray-Level Emphasis		
Gray-Level Variance		
Zone-Size Variance		
Spatial Frequency		

The bold face image features are the ten best image features.
[*]*Homogeniety (GLCM) was seleceted for both d = 2 and 4.*

The MDS scatter graph of the perceptual space, in Fig. 4, shows distinctive trends and groupings, i.e., perceptually similar samples are clustered together. The scattering of the samples in the perceptual space follow a horseshoe curve. The roughest samples occupy the right side of the curve in the graph and as we move along the curve towards the left side, the roughness of the samples gradually decrease. Additionally, the curve exhibits some width also. The inner side tends to have softer samples as compared to the outer side .

It can be seen that the sandpaper samples which are distinctly different from all other surfaces, are located in a separate group in the right top corner of the graph. All other samples are located along a continuum. On one end, it starts with the surfaces having visible contours, e.g., steel and plastic meshes etc. These were deemed as the roughest samples. Next are the surfaces which have a visibly rough surface e.g., towel, carpet etc. The middle of the horseshoe curve is occupied by the mildly textured surfaces, most of them being fabrics. They include, cloth-hard-cover, jeans, fine sand paper etc. The other end of the horseshoe contains the smooth surfaces. Smooth surfaces are smooth shoe padding, aluminum, acrylic etc.

4 IMAGE FEATURE SPACE

In the image feature space, the visual texture of a surface is represented as a multidimensional feature vector calculated from an image of the surface. A total of 98 image features were calculated from each surface using well known image feature extraction techniques, constructing a 98 dimensional

vector. The details of all the image features used in this study can be found in Table 1.

4.1 Image Capturing Setup

The finer details of image depend on the scale and resolution of the image. In an effort to remove the effects of scaling and resolution, all the images were captured with the same camera (SIGMA Digital Camera dp2 Quattro). The camera was mounted on a tripod and placed directly over the surface. The distance from the camera to the surface was kept constant at 300 mm. Standard room lighting was used during the capturing process. However, special care was taken to guard against any shadows in the images. The images were captured in high quality RAW format (loss less compression, 14-bit). The images were cropped to a size of 300×300 pixels. The images were also converted to gray scale in order to make them color independent.

4.2 Image Feature Selection

Given the large size of the image feature vector, it was infeasible to use all the features for prediction of perceptual haptic texture. Therefore, the most correlated image features with the MDS dimensions were selected through a sequential forward selection (SFS) algorithm. Afterwards, these features were put through a parallel analysis test to check if the resulting correlation values in the SFS are achieved by chance or they bare some significance. Features with the best predictive ability were highlighted as a result of parallel analysis. The feature selection process is shown in Fig. 6.
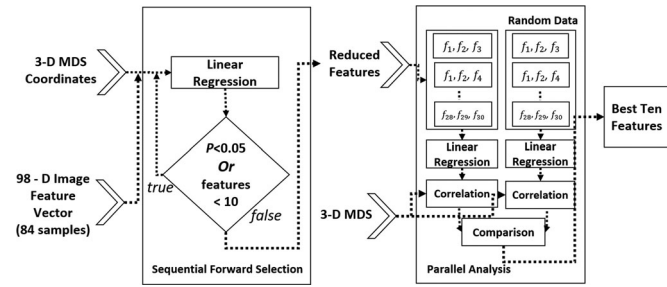
Fig. 6. The two step process used for feature selection. Sequential forward selection reduces image feature vector from 98 to 30 dimensions based on correlation with perceptual space. Parallel analysis provides the ten most correlated and significant features among the given 30.

4.2.1 Sequential Forward Selection

A sequential forward selection algorithm [46] was applied to reduce the dimension of the image feature vector (98 features). The input to the algorithm is the 98 dimensional image feature vector and the coordinate values of the first three dimensions given by MDS. For every single MDS dimension, the algorithm starts with the most correlated image feature and predicts the output. The output is in the form of the MDS dimension. A linear regression model was used to predict the output. Then it adds a second feature and predicts the output once again. It keeps on adding features until the termination criterion is met. The termination criterion in this case was either of, the prediction error being significantly reduced $p \geqslant 0.05$, (using partial F-test) or a total of ten image features being selected for each dimension. The number ten was empirically determined. For all the dimensions, the prediction error was never significantly reduced for the first ten features. Thus, we had a reduced feature set of 30 distinct image features, ten per dimension. Repetition of features occurred once we selected more than ten features per dimension. Increase in number of features also reduces the efficiency of the system due to curse of dimensionality. Therefore, ten features were considered as sufficient to explain the variations along a single dimension.

4.2.2 Parallel Analysis

Parallel analysis [47], [48] is carried out to see if the image feature is really related to the perceived haptic texture and to examine the predictability of the reduced feature compared to that of a random data set with the same dimensions. Our hypothesis is that the predictability of the reduced image feature subset should be higher than that of random data.

For the analysis, the reduced image feature subset of 30 image features was further divided into all possible subsets of three image features. The predictive quality of every subset was evaluated for the first three MDS dimensions using linear regression. The output from regression was the MDS coordinate values of the corresponding dimension. Subsequently, the correlations between the predicted values and the actual MDS coordinate values were measured.

The same process was repeated for a randomly generated data matrix which was of the same dimension as the reduced image feature vector. The correlations between the predicted output from random data subsets and actual MDS coordinate values were also recorded.
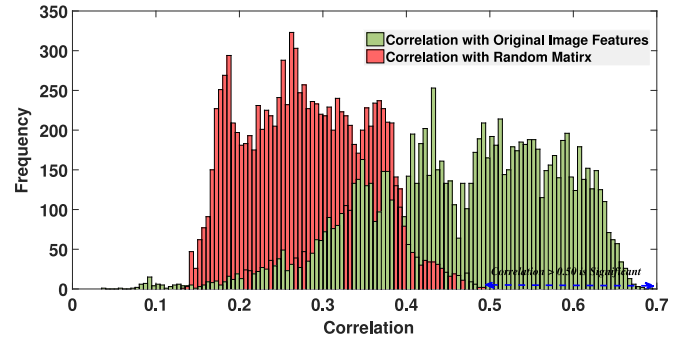

Fig. 7. Correlation values for the image feature subsets and the randomly generated data subsets with the first three MDS dimensions.

The correlation values measured from the randomly generated matrix are the values that can be achieved by chance and have no significance. Therefore, only those image feature subsets are significant which showed correlation values higher than the maximum correlation from randomly generated data. Fig. 7 shows the correlation values for the image feature subsets (see green bars) and the randomly generated data (see red bars).

The maximum correlation for a random data subset was 0.47. To be on the safer side, a value of 0.50 was considered. Image feature subsets with correlation higher than 0.50 were considered as significant. The frequency of features constituting the significant image feature subsets was calculated. The best features were the ones which occurred most frequently in the significant feature subsets. The ten features with the highest frequency were: Gray-level non-uniformity (GLRLM); gray-level non-uniformity and small Zone High Gray-level emphasis (GLSZM); gradient percentile 25 percent (Gradient); correlation, homogeneity, information measure of correlation (2), and inverse difference moment normalized (GLCM at d = 4); homogeneity and information measure of correlation (1) (GLCM at d = 2). These features were selected for the automatic haptic model assignment algorithm discussed in Sections 5 and 6.

4.3 Description of the Selected Image Features

This section provides a brief overview of the ten image features obtained as a result of the image feature selection process.

The GLCM is a matrix which considers the spatial relationships between two pixels at a time in the image. *Correlation* measures the linear dependency of grey levels on those of neighboring pixels. *Homogeneity* measures image homogeneity as it assumes larger values for smaller gray tone differences in pair elements. The weights decrease exponentially away from the diagonal. *Inverse difference moment normalized* is a linear measure which calculates the gray tone differences among pixels. *Information measure of correlation 1 and 2* are statistically derived from the correlation measure. The GLRLM looks at runs of pixels, rather than looking at pairs of pixels, i.e., how many pixels of a given grey value occur in a sequence in a given direction. *Gray level non-uniformity* measures the similarity of gray level intensity values in the run length matrix. The GLSZM looks at zones of connected pixels, i.e., how many pixels of a given grey value are connected in a single group. *Gray level non-uniformity* measures the similarity of gray level intensity
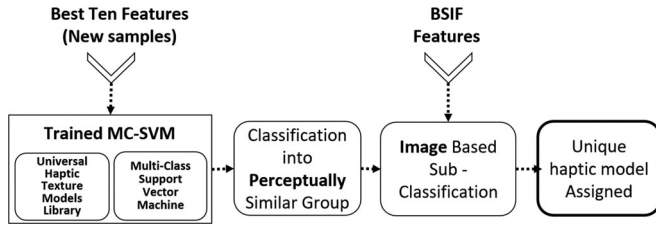
Fig. 8. The process of assigning haptic models to newly encountered textures.

values in the size zone matrix. *Small zone high gray level emphasis* is a robust and highly discriminative statistical measure since it includes the pixel information in addition to the rows and columns of the size zone matrix. The *25 percentile* gives the highest peak under which 25 percent of the pixels are in the image.

5   RELATIONSHIP BETWEEN PERCEPTUAL HAPTIC TEXTURE SPACE AND IMAGE FEATURE SPACE

Fig. 4 shows that the scatter graph of haptic perceptual space exhibits distinct grouping of perceptually similar samples while in Section 4, it was shown that there exists a relation between the image feature space and the haptic perceptual space. Based on this knowledge, it is assumed that the image feature space could also be classified into groups of haptic-perceptually similar images. For this purpose, a Multi-Class Support Vector Machine (MC-SVM) [49] was used in conjunction with K-means clustering [50].

Since the distribution of groups in image feature space cannot be predicted, a one-versus-rest Multi-Class Support Vector Machine (SVM) algorithm with a Radial Basis Function (RBF) kernel was used for clusterizing the image feature space. The use of RBF kernel was preferred since it can handle both linearly separable as well as inseparable data. Data in which clusters cannot be distinguished linearly is called as linearly inseparable. The multi-class SVM algorithm was tested for different values of the parameter sigma, and the best results were obtained at sigma = 4. Another possibility was to use deep learning as it is used in various research areas and could provide better results, but in this case it was not applicable due to the limited size of our dataset. Similarly, other algorithms were also tried for the classification, however, MC-SVM provided the best results for our dataset. On the other hand, the clusterization of perceptual space was carried out using k-means algorithm. This clusterization falls under the umbrella of unsupervised learning, and k-means is one of the most powerful algorithm for unsupervised learning.

The reduced image feature set (ten image features) for all the 84 samples was used as input for training the MC-SVM. To provide labels for the SVM, k-means clusterization was applied to the haptic perceptual space. The labels are used to classify different samples into perceptually similar groups. As shown in Fig. 4, perceptually similar samples are in close proximity with one another. Therefore, as a result of the k-means classification, perceptually similar samples were grouped together. Since the overall range of samples used in this study can subjectively be divided into 16 broad categories, the number of groups used in k-means was decided to be 16. This grouping can be seen in Fig. 4. The imbalance in

the variance of the groups increases if the total number of groups are increased beyond 16. While, a lower number of total groups results in perceptually different surfaces being grouped together. As a result, the image features were labeled from perceptual clusterization and the MC-SVM was trained on this data. Consequently, a *Haptic Texture Library* was formed where image features of texture surfaces were directly associated with the perceptual haptic texture of the surfaces. The trained model of MC-SVM was used to classify new texture surfaces to perceptually similar groups based on the image features of the new surface.

6   AUTOMATIC HAPTIC MODEL ASSIGNMENT

The relationship established between image feature space and the perceptual haptic texture space was used to automatically assign haptic models to newly encountered textured surfaces. The automatic haptic model assignment was a two-step process. First, the trained MC-SVM model was used to assign a perceptually similar group to the new sample based on its image features. Second, an exact match within the selected perceptually similar group was assigned based on an image classification technique, known as Binarized Statistical Image Features (BSIF) [32]. BSIF is a local image descriptor specifically designed for encoding texture information. It differs from other descriptors in the type of filters used for convolution. Usually, these filters are manually predefined, whereas, in BSIF, these filters are learnt from statistics of natural images. Since the surfaces used in this study can also be considered as natural, BSIF provides better modeling capacity as compared to other descriptors. The overall framework for automatic haptic model assignment is shown in Fig. 8.

The trained SVM model was used to assign a perceptually similar haptic model from the library to a new real life texture surface. As a first step, the reduced image feature set was calculated for the new sample. This image feature set was used as a test input to the SVM model. The trained SVM model then classified the new sample into one of the groups, which were made in Section 5.

As a pre-process to the second step, binarized statistical image features were calculated for all the surfaces in the perceptual space. In the second step, BSIF features were calculated for the new sample and compared to other samples within the group selected in the first step. The comparison was carried out using chi-squares distances. The haptic model of the sample, within the selected group, having the lowest distance to the new sample was assigned to it.

7   PERFORMANCE EVALUATION

A psychophysical experiment was conducted for evaluation of the automatic assignment. The experiment was conducted to check if the haptic model assigned by the algorithm is perceptually similar to the new sample. The new sample over here is the surface to which we wanted to assign a haptic model using our algorithm.

7.1   Experiment

The design of the evaluation experiment was a cluster sorting task similar to the one conducted in Section 3. The aim
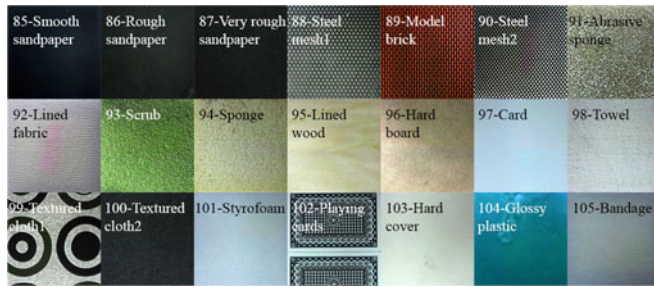
Fig. 9. The 21 new textured surfaces used for evaluation.

of this experiment was to validate the authenticity of the automatic assignment algorithm. For this purpose, 21 new outside-library samples were used and the automatic assignment algorithm was used to assign them haptic models from the library. In the experiment, the 21 new samples in addition to the earlier 84 surfaces were used and participants were asked to classify them into perceptually similar groups. A perceptual space having these 105 samples was built using MDS. This provided us ground truth data about the 21 new samples in terms of their location in perceptual space. Afterwards, the automatic assignment algorithm was also used to assign haptic models to the new surfaces. If the model assigned by the algorithm appeared in the same perceptual group as in the experiment, the assignment was considered to be correct. The details of the experiment are provided in the following sections.

7.1.1 Participants and Stimuli

A total of six participants took part in the experiment. None of the participants were part of the initial experiment for building the perceptual haptic texture space. The participants reported no disabilities and had never been part of such an experiment. They were paid for their participation.

The stimuli for the evaluation experiment were a set of 105 real life textured surfaces. The 84 samples used in Section 3 and a new set of 21 real life textured samples constituted the 105 samples. Each sample was mounted on an acrylic plate of size $100 \times 100 \times 5$ mm. Fig. 9 shows the new set of 21 samples.

7.1.2 Procedure

The experiment was a cluster sorting task where the participants were asked to classify perceptually similar samples into groups. A total of three trials were conducted per participant, and the number of groups in these trials were 6, 9, and 12. The number of groups in a particular trial were randomly selected to avoid any bias. The rest of the details of the experiment were the same as the previous experiment.

7.1.3 Data Analysis and Results

The data from the experiment was converted into a dissimilarity matrix and scaled from 0 to 1000. The dissimilarity values were calculated in the same way as in the initial experiment in Section 3. MDS analysis was performed on the dissimilarity matrix. The kruskal stress value for the first ten dimensions is shown in Fig. 5. The stress value for three dimensions is 0.062, which is considered as fair according to [38]. Therefore, a three dimensional space was established

to visualize the new samples in relation to the old samples. The space obtained as a result of MDS analysis was also divided into 16 perceptually similar groups using K-means. The scatter graph of the new space can be seen in Fig. 10.

7.2 Evaluation Criterion

On one hand, the automatic haptic model assignment algorithm was used to assign haptic models to the new samples based on their image features. On the other hand, in the experiment, the participants classified the new samples into different groups along with the old samples. After applying K-means to the new space, all the samples were classified into perceptually similar groups. The new samples also appeared in these groups along side the old ones. These groups would provide the ground truth for the automatic haptic model assignment algorithm. An automatic assignment of a haptic model would be deemed as correct only if both the new sample and the corresponding assigned model appeared in the same perceptual group in the new space.

The haptic models assigned to all the new samples were evaluated based on the above strategy. A total of 15 out of the 21 new samples were assigned perceptually correct models i.e., the new samples and corresponding assigned model appeared in the same perceptual group. The haptic models assigned to the 21 new samples are presented in Table 2. Fig. 10 shows the new samples and the corresponding assigned models inside the new perceptual space.

After checking for the correct perceptual group assignment, it was important to check if the assigned models and new samples appear closer to each other inside a group. This was checked in relation to the overall variance of the groups. The average normalized variance of all the groups was 0.24 units in perceptual space. Based on this variance, the new samples having smaller distances as compared to average variance are considered as perceptually very similar to their assigned model. The histogram in Fig. 11 shows that the majority of samples exhibit far less distances as compared to average variance. This means that the majority of assigned models are perceptually very similar to the new surfaces.

7.3 Comparison between the 84-Surface and 105-Surface Perceptual Spaces

Figure 12 shows the comparison between the perceptual spaces for 84 surfaces and 105 surfaces. The perceptual spaces are represented in two dimensional cross sections for better visualization for comparison purposes. To remove scaling artifacts, both the spaces were scaled from zero to one. All three dimensions of both the spaces largely follow the same trends. Especially, the first two dimensions exhibit remarkable similarity. This shows that the addition of 21 new surfaces did not alter the basic shape of the perceptual space. The new surfaces either fitted inside or lie immediately outside the boundary of the convex hull created by the original 84 surfaces.

Both spaces were divided into 16 clusters having variable number of surfaces in each cluster. After examining the clusters, it was evident that most of the groups largely carried the same surfaces in both the perceptual spaces. Only 11 (out of the original 84) surfaces in the 105-surfaces perceptual space, residing on the cluster boundaries, had jumped into the adjoining clusters. this behavior was expected since
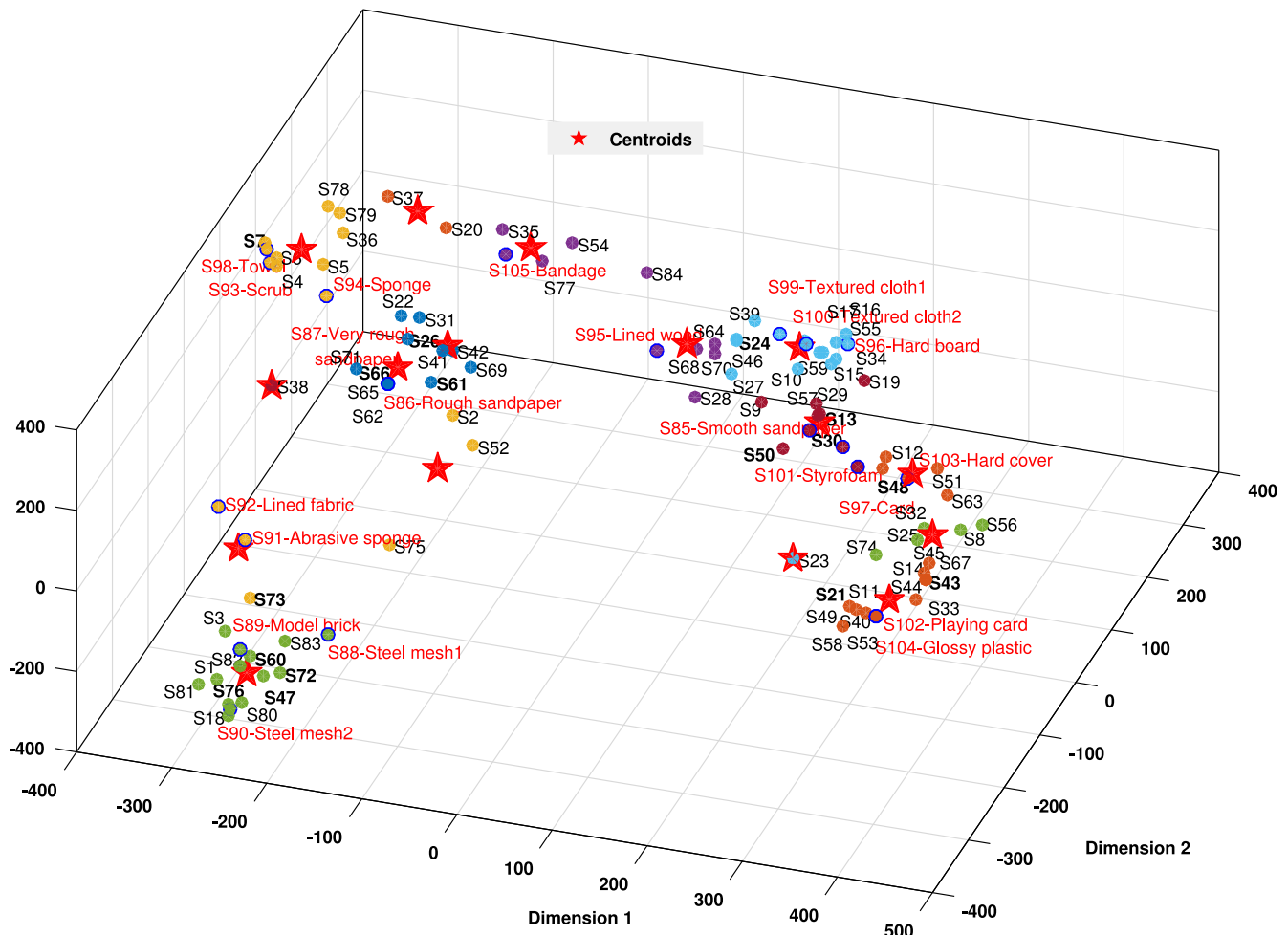
Fig. 10. The new perceptual space made up of 21 new and 84 old texture surfaces. The different colors (of circles) represent the different groups as a result of K-means clustering. The stars show the centroids of these groups. The new surfaces are written in red color while the assigned models are shown in bold black color.

multidimensional scaling and kmeans optimize each point in the space. However, it must be noted that the haptic library is established based on the 84-surface perceptual space and the 105-surface perceptual space was established for evaluation purposes only, i.e., to check if the new surface and its assigned surface resided in the same group.

8 DISCUSSION

From Fig. 10, it can be seen that texture surfaces having visible rough texture (S88-Steel mesh1, S89-Model brick, S90-Steel mesh2 etc.) or the ones having some degree of roughness in texture (S86-Rough sandpaper, S87-Very rough sandpaper, S93-Scrub etc) are quite accurately classified. The image features from these surfaces were very clear and the algorithm could readily differentiate the surfaces from one another. On the other hand, the smooth surfaces (S102-Playing card, S104-Glossy plastic) were incorrectly classified due to the fact that the images captured from these surfaces could not portray the surface micro geometry. This can be accredited to the limitation of hardware since the camera could not capture the surface details for these texture surfaces. Thus the image features from these surfaces were not clear and the algorithm classified them incorrectly.

Another set of surfaces that was wrongly classified was the set of textured cloth2 (S100) and lined wood (S95). The

algorithm assigned a moderately rough sandpaper (S66) to textured cloth2 (S100). Upon a closer inspection it was revealed that the actual surface texture of the two surfaces was quite similar and that the two should have been assigned to the same group by the human subjects, while building the actual perceptual space. Same was the case for lined wood (S95) to which the algorithm assigned S73 (kite paper). These two also resemble each other and should have been placed in the same group.

After careful deliberation on the experimental process it was noted that since S66 was a sandpaper and as soon as it was encountered, human subjects would directly assign it to the group where other sandpapers were previously placed. This assignment usually took place without considering the actual surface details, instead the basis for assignment were the material properties of the surface. Additionally, sandpapers have a very peculiar surface and are easily recognizable. This fact also aided the material based assignment process. At the same time, textured cloth2 (S100) was equally rough but it was a fabric. The fact that it was a fabric played a major role in it being assigned to a completely different group as compared to the given sandpaper.

The phenomenon where surfaces are classified based on their material properties instead of actual textural

TABLE 2
Haptic Texture Models Assigned to the
21 New Texture Surfaces

New Texture Surface	Assigned Model	Remarks	Distance from Assigned Model (normalized 0-1)
85	30	Correct	0.05
86	26	Correct	0.07
87	61	Correct	0.04
88	47	Correct	0.09
89	60	Correct	0.01
90	76	Correct	0.02
91	73	Correct	0.07
92	73	Correct	0.12
93	7	Correct	0.04
94	7	Correct	0.14
95	73	Wrong	0.52
96	21	Wrong	0.86
97	50	Correct	0.13
98	7	Correct	0.01
99	24	Correct	0.08
100	66	Wrong	0.61
101	13	Correct	0.10
102	72	Wrong	0.95
103	48	Correct	0.06
104	61	Wrong	0.88
105	43	Wrong	0.92
Classification accuracy		**71.4%**	

Fig. 12. Comparison between 2-dimensional cross sections of the 3D perceptual spaces for 84 and 105 surfaces.

surface (among the library surfaces) would be perceptually dissimilar to the test surface.

In case of a surface containing artificial patterns, the success or failure of the algorithm depends on topography of the surface. If the artificial patterns are significant enough to mask the topography (or the surface is too smooth for the camera to capture the topography), the algorithm would fail to assign a perceptually similar surface. The playing cards (S102) is an example of this phenomenon. On the other hand, if the surface exhibits camera visible texture, the algorithm can successfully assign a perceptually similar surface from the library. For instance textured cloth1 (S99) was successfully classified despite having artificial patterns. It contains visible micro geometry which was readily detected by the camera and the algorithm could assign a perceptually correct model from the library.

It can be noted that the psychophysical experiment to establish the perceptual space is based on bare-handed interaction with the surfaces. The participants rated the dissimilarities between different surfaces by directly interacting with the surfaces using their hands. This data played a significant role in formulating the automatic assignment algorithm. On the other hand, most haptic rendering and modeling algorithms consider a tool-based interaction with the surfaces. It can be argued that this difference in mode of interaction might cause different perceptual sensations. However, in our previous study it was shown that the sensations perceived through bare-handed and tool-based interactions are largely similar [51]. It is also highlighted that the different dimensions for both types of interactions bare a high degree of correlation. Thus, in most cases the classifications provided by the automatic assignment algorithm will readily translate into perceptually correct haptic models for tool-based haptic modeling and rendering environments. On the other hand, it is possible that the difference in modes of interaction can result in a misclassification by the automatic assignment algorithm. These errors, as mentioned earlier, can originate due to the pre-judgement phenomenon.

Here we would like to state that the textures used in [51] were a subset of the textures used in this study. The perceptual space in [51] showed four dimensions, while the perceptual space in the current study comprises of only three dimensions. Upon a closer inspection it becomes evident that one of the four dimensions in [51] was related to hardness-softness, which is not considered in this study. Although adjective rating analysis of the current perceptual space has not being carried out in this study, as the scope of this article is different, it is safe to assume that the three dimensions of the current perceptual space should relate highly with the dimensions highlighted in [51].

differences is called as *Pre-Judgement* in [51]. In pre-judgment participants use their previous knowledge for classifying a surface. A similar scenario developed for the lined wood (S95) and kite paper (S73) pair, where S95 was a wood (classic case of pre-judgement) and S73 was a kite paper.

The database of surfaces used in this study mostly comprises of everyday office/household materials. Furthermore, the texture of the surfaces was uniform and natural to a large extent. Similarly, the 21 surfaces used for evaluation also exhibited roughly the same properties. However, in real life we encounter a multitude of surfaces which are not represented in the current study. For example, organic surfaces, oily or wet surfaces, surfaces with artificial patterns, etc. Thus, it can be said that the current library covers some portion of the overall haptic space. Keeping this in mind, if we test a surface which belongs to the same portion of the overall haptic space as the library, the assigned model would mostly be perceptually similar. However, if we test a surface which lies far away from the library surfaces in the haptic space, the assigned model despite being the closest
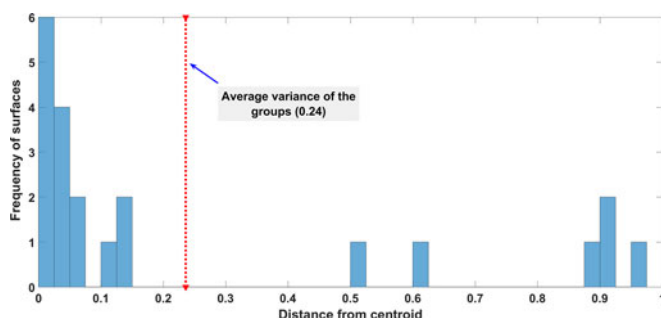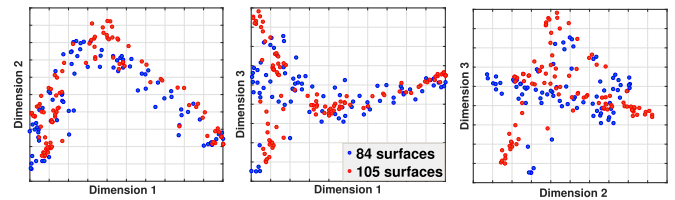

Fig. 11. Histogram of the distances between new surfaces and the assigned haptic models from the library.

Image feature extraction is one of the core parts of the current system. During the course of this research it was found that the image capturing process should be deliberated carefully. The image capturing mechanism should be robust and repeatable in order to extract meaningful image features. Especially, the lighting conditions and clarity of texture play a vital role. The images should be captured with a good quality camera in good lighting conditions.

9 CONCLUSION

Our research concludes that visual features extracted from the image, if carefully selected, can reveal important physical characteristics related to perceptual haptic surface texture. Based on this relation, perceptual haptic models library was established and haptic models were assigned automatically to a given surface. The proposed system showed reasonable accuracy in assigning perceptually similar haptic texture models. This research can help in standardization and simplification of the haptic texture modeling and rendering process. It can eliminate the need for building a haptic model for every surface, instead, a perceptually similar model can be assigned to a given surface from the library.

ACKNOWLEDGMENTS

REFERENCES

[1] D. C. Ruspini, K. Kolarov, and O. Khatib, "The haptic display of complex graphical environments," in *Proc. 24th Annu. Conf. Comput. Graph. Interactive Techn.*, 1997, pp. 345–352.

[2] S. Jeon and S. Choi, "Real stiffness augmentation for haptic augmented reality," *Presence: Teleoperators Virtual Environ.*, vol. 20, no. 4, pp. 337–370, 2011.

[3] T. Yamamoto, B. Vagvolgyi, K. Balaji, L. L. Whitcomb, and A. M. Okamura, "Tissue property estimation and graphical display for teleoperated robot-assisted surgery," in *Proc. IEEE Int. Conf. Robot. and Autom.*, 2009, pp. 4239–4245.

[4] A. M. Okamura, M. R. Cutkosky, and J. T. Dennerlein, "Reality-based models for vibration feedback in virtual environments," *IEEE/ASME Trans. Mechatronics*, vol. 6, no. 3, pp. 245–252, Sep. 2001.

[5] R. Hover, G. Kósa, G. Székely, and M. Harders, "Data-driven haptic rendering from viscous fluids to visco-elastic solids," *IEEE Trans. Haptics*, vol. 2, no. 1, pp. 15–27, Jan.-Mar. 2009.

[6] P. Fong, "Sensing, acquisition, and interactive playback of data-based models for elastic deformable objects," *Int. J. Robot. Res.*, vol. 28, no. 5, pp. 630–655, 2009.

[7] M. Mahvash and V. Hayward, "High-fidelity haptic synthesis of contact with deformable bodies," *IEEE Comput. Graph. Appl.*, vol. 24, no. 2, pp. 48–55, Mar.-Apr. 2004.

[8] S. Andrews and J. Lang, "Haptic texturing based on real-world samples," in *Proc. Int. Workshop Haptic Audio Visual Environ. Games*, 2007, pp. 142–147.

[9] H. Culbertson, J. Unwin, and K. J. Kuchenbecker, "Modeling and rendering realistic textures from unconstrained tool-surface interactions," *IEEE Trans. Haptics*, vol. 7, no. 3, pp. 381–393, Jul.-Sep. 2014.

[10] H. Vasudevan and M. Manivannan, "Recordable haptic textures," in *Proc. IEEE Int. Workshop Haptic Audio Visual Environ. Their Appl.*, 2006, pp. 130–133.

[11] S. S. Wall and W. S. Harwin, "Modelling of surface identifying characteristics using fourier series," in *Proc. Winter Annu. Meet. ASMEDSC - ASME Dynamic Syst. Control Division*, 1999, pp. 65–71.

[12] A. Abdulali and S. Jeon, "Data-driven modeling of anisotropic haptic textures: Data segmentation and interpolation," in *Proc. Int. Conf. Human Haptic Sens. Touch Enabled Comput. Appl.*, 2016, pp. 228–239.

[13] A. Abdulali and S. Jeon, "Data-driven rendering of anisotropic haptic textures," in *Proc. Int. Asia Haptics Conf.*, 2016, pp. 401–407.

[14] K. E. MacLean, "The haptic camera: A technique for characterizing and playing back haptic properties of real environments," in *Proc. Haptic Interfaces Virtual Environ. Teleoperator Syst.*, 1996, pp. 459–467.

[15] L. Kim, G. S. Sukhatme, and M. Desbrun, "Haptic editing of decoration and material properties," in *Proc. 11th Symp. Haptic Interfaces Virtual Environ. Teleoperator Syst.*, 2003, pp. 213–220.

[16] S. J. Lederman and S. G. Abbott, "Texture perception: Studies of intersensory organization using a discrepancy paradigm, and visual versus tactual psychophysics," *J. Exp. Psychology: Human Perception Performance*, vol. 7, no. 4, pp. 902–915, 1981.

[17] J. Eck, A. L. Kaas, and R. Goebel, "Crossmodal interactions of haptic and visual texture information in early sensory cortex," *Neuroimage*, vol. 75, pp. 123–135, 2013.

[18] M. O. Ernst and M. S. Banks, "Humans integrate visual and haptic information in a statistically optimal fashion," *Nature*, vol. 415, no. 6870, pp. 429–433, 2002.

[19] M. Yoshida, "Dimensions of tactual impressions (1)," *Japanese Psychological Res.*, vol. 10, no. 3, pp. 123–137, 1968.

[20] M. Hollins, S. Bensmaïa, K. Karlof, and F. Young, "Individual differences in perceptual space for tactile textures: Evidence from multidimensional scaling," *Perception Psychophysics*, vol. 62, no. 8, pp. 1534–1544, 2000.

[21] S. Okamoto, H. Nagano, and Y. Yamada, "Psychophysical dimensions of tactile perception of textures," *IEEE Trans. Haptics*, vol. 6, no. 1, pp. 81–93, Jan.-Mar. 2013.

[22] D. Picard, C. Dacremont, D. Valentin, and A. Giboreau, "Perceptual dimensions of tactile textures," *Acta Psychologica*, vol. 114, no. 2, pp. 165–184, 2003.

[23] H. Shirado and T. Maeno, "Modeling of human texture perception for tactile displays and sensors," in *Proc. IEEE 1st Joint Eurohaptics Conf. Symp. Haptic Interfaces Virtual Environ. Teleoperator Syst. World Haptics Conf.*, 2005, pp. 629–630.

[24] R. H. LaMotte, "Softness discrimination with a tool," *J. Neurophysiology*, vol. 83, no. 4, pp. 1777–1786, 2000.

[25] M. Hollins, F. Lorenz, A. Seeger, and R. Taylor, "Factors contributing to the integration of textural qualities: Evidence from virtual surfaces," *Somatosensory Motor Res.*, vol. 22, no. 3, pp. 193–206, 2005.

[26] R. Klatzky, S. Lederman, C. Hamilton, and G. Ramsay, "Perceiving roughness via a rigid probe: Effects of exploration speed," in *Proc. ASME Dynamic Syst. Control Division*, vol. 67, pp. 27–33, 1999.

[27] M. A. Heller, "Visual and tactual texture perception: Intersensory cooperation," *Perception Psychophysics*, vol. 31, no. 4, pp. 339–344, 1982.

[28] R. M. Haralick, et al., "Textural features for image classification," *IEEE Trans. Syst. Man Cybernet.*, no. 6, pp. 610–621, Nov. 1973.

[29] V. Arvis, C. Debain, M. Berducat, and A. Benassi, "Generalization of the cooccurrence matrix for colour images: Application to colour texture classification," *Image Anal. Stereology*, vol. 23, no. 1, pp. 63–72, 2011.

[30] T. Ojala, M. Pietikainen, and T. Maenpaa, "Multiresolution grayscale and rotation invariant texture classification with local binary patterns," *IEEE Trans. Pattern Anal. Mach. Intell.*, vol. 24, no. 7, pp. 971–987, Jul. 2002.

[31] L. Liu and P. Fieguth, "Texture classification from random features," *IEEE Trans. Pattern Anal. Mach. Intell.*, vol. 34, no. 3, pp. 574–586, Mar. 2012.

[32] J. Kannala and E. Rahtu, "Bsif: Binarized statistical image features," in *Proc. IEEE 21st Int. Conf. Pattern Recognit.*, 2012, pp. 1363–1366.

[33] M. Strese, J.-Y. Lee, C. Schuwerk, Q. Han, H.-G. Kim, and E. Steinbach, "A haptic texture database for tool-mediated texture recognition and classification," in *Proc. IEEE Int. Symp. Haptic Audio Visual Environ. Games*, 2014, pp. 118–123.

[34] J. M. Romano and K. J. Kuchenbecker, "Methods for robotic tool-mediated haptic surface recognition," in *Proc. Haptics Symp.*, 2014, pp. 49–56.

[35] M. Strese, C. Schuwerk, A. Iepure, and E. Steinbach, "Multimodal feature-based surface material classification," *IEEE Trans. Haptics*, vol. 10, no. 2, pp. 226–239, Apr.-Jun. 2017.

[36] J. Pasquero, J. Luk, S. Little, and K. MacLean, "Perceptual analysis of haptic icons: An investigation into the validity of cluster sorted mds," in *Proc. 14th Symp. Haptic Interfaces Virtual Environ. Teleoperator Syst.*, 2006, pp. 437–444.

[37] M. Hollins, R. Faldowski, S. Rao, and F. Young, "Perceptual dimensions of tactile surface texture: A multidimensional scaling analysis," *Perception Psychophysics*, vol. 54, no. 6, pp. 697–705, 1993.

[38] J. B. Kruskal, "Multidimensional scaling by optimizing goodness of fit to a nonmetric hypothesis," *Psychometrika*, vol. 29, no. 1, pp. 1–27, 1964.

[39] F. Wickelmaier, "An introduction to MDS," Sound Quality Res. Unit, Aalborg University, Denmark, 2003, Art. no. 46.

[40] M. M. Galloway, "Texture analysis using gray level run lengths," *Comput. Graph. Image Process.*, vol. 4, no. 2, pp. 172–179, 1975.

[41] A. Chu, C. M. Sehgal, and J. F. Greenleaf, "Use of gray value distribution of run lengths for texture analysis," *Pattern Recognit. Lett.*, vol. 11, no. 6, pp. 415–419, 1990.

[42] B. V. Dasarathy and E. B. Holder, "Image characterizations based on joint gray level-run length distributions," *Pattern Recognit. Lett.*, vol. 12, no. 8, pp. 497–502, 1991.

[43] G. Thibault, et al., "Texture indexes and gray level size zone matrix application to cell nuclei classification," in *Proc. Pattern Recognit. Inf. Process.*, 2009, pp. 140–145.

[44] D. A. Clausi, "An analysis of co-occurrence texture statistics as a function of grey level quantization," *Canadian J. Remote Sensing*, vol. 28, no. 1, pp. 45–62, 2002.

[45] M. Amadasun and R. King, "Textural features corresponding to textural properties," *IEEE Trans. Syst., Man and Cybern.*, vol. 19, no. 5, pp. 1264–1274, Sep./Oct. 1989.

[46] R. Kohavi and G. H. John, "Wrappers for feature subset selection," *Artif. Intell.*, vol. 97, no. 1, pp. 273–324, 1997.

[47] B. Thompson and L. G. Daniel, "Factor an alytic evidence for the construct validity of scores: A historical overview and some guidelines," *Educ. Psychological Meas.*, vol. 56, no. 2, pp. 197–208, 1996.

[48] J. C. Hayton, D. G. Allen, and V. Scarpello, "Factor retention decisions in exploratory factor analysis: A tutorial on parallel analysis," *Organizational Res. Methods*, vol. 7, no. 2, pp. 191–205, 2004.

[49] J. Weston and C. Watkins, "Multi-class support vector machines," Citeseer, Tech. Rep., 1998.

[50] D. Arthur and S. Vassilvitskii, "k-means++: The advantages of careful seeding," in *Proc. 18th Annu. ACM-SIAM Symp. Discrete Algorithms*, 2007, pp. 1027–1035.

[51] W. Hassan and S. Jeon, "Evaluating differences between barehanded and tool-based interaction in perceptual space," in *Proc. IEEE Haptics Symp.*, 2016, pp. 185–191.

Muhammad Abdullah received the BS degree in electrical engineering from the National University of Science and Technology (NUST), Pakistan. Currently, he is working towards the MS degree in the Department of Computer Science and Engineering, Kyung Hee University, Republic of Korea. His current research interests include encountered-type haptics devices and virtual reality.

Sang Chul Ahn received the MSc and PhD degrees in control and instrumentation from Seoul National University, in 1990 and 1996, respectively. He was a visiting scholar in the Computer Science Department, USC, in 1996. He has been with KIST since 1997. Now, he is a principal researcher in the Center for Imaging Media Research, RMI, KIST. He is also the chief professor of the Division of Nano and Information Technology at the UST KIST School, Korea. He is a member of the IEEE and ACM. His main research interests are vision based human computer interaction, mixed reality, image based modeling/rendering, and robotics.

Seokhee Jeon received the BS and PhD degrees in computer science and engineering from the Pohang University of Science and Technology (POSTECH), in 2003 and 2010, respectively. He was a postdoctoral research associate in the Computer Vision Laboratory, ETH Zurich. In 2012, he became an assistant professor in the Department of Computer Engineering, Kyung Hee University. His research focuses on haptic rendering in an augmented reality environment, applications of haptics technology to medical training, and usability of augmented reality applications. He is a member of the IEEE.

Waseem Hassan received the BS degree in electrical engineering from the National University of Science and Technology (NUST), Pakistan, and the MS degree in computer engineering from Kyung Hee University, Republic of Korea. Currently, he is working towards a doctoral degree in the Department of Computer Science and Engineering, Kyung Hee University. His research interests include psychophysics, and haptic texture perception and augmentation.

Arsen Abdulali received the BS degree in computer engineering from the Tashkent University of Information Technologies, Uzbekistan. Currently, he is working toward the PhD degree in the Department of Computer Science and Engineering, Kyung Hee University, Republic of Korea. His research focus lies in data-driven haptic texture modeling and rendering.